Modelling Higher Dimensional Chaos with a Time-Delayed Map

Frederick H. Willeboordse

July 14, 1992

Institute of Physics [1], *University of Tsukuba, Ibaraki 305, Japan*

Abstract

It will be shown that many phenomena, that so far were considered to be purely spatio-temporal, can be obtained with the help of a recently introduced Time-Delayed Map and only one (chaotic) element. This is achieved by applying a space-time rotation to a Coupled Map Lattice. Applications to one and two dimensional systems will be given. A new correlation function that can be used to extract spatial information from a time series is introduced.

[1] e-mail: frederik@panque.ph.tsukuba.ac.jp

One of the approaches to efficiently study the phenomenology of complex systems is to construct a discrete spatially extended system. The Coupled Map Lattice (CML) [1,2] which includes space in a direct and comprehensible way by coupling local elements, has become one of the standard models in the study of higher dimensional chaos in recent years.

It is well known that delay differential equations can display high dimensional characteristics [3]. It is to be expected then that this is also true for discrete Time-Delayed Maps (TDM). The special feature of the the TDMs introduced in [4,5,6] is that, in many cases, their phenomenology is either identical or very similar to that of a CML.

Thus, apart from being interesting in its own right, the TDM might be useful for gainig a better understanding of a CML. Especially, the conceptually slightly less transparent but, due to the lack of boundary conditions, mathematically more straigthforward coupling algorithm might simplify theoretical analysis. Furthermore, the TDM might be helpful for understanding the relationship between maps with a delay or a memory term and a CML. Recently, it was e.g. shown that under certain circumstances a map with a memory term can relax onto an unstable fixed point [7]. In difffusively coupled logistic maps, a Pattern Selection regime is well known to exist in parameter regions where the single logistic map is chaotic and accordingly possesses an infinite number of unstable orbits.

Since a TDM generates a time series, and the close relation of the TDM and the CML is known a priori, it would be interesting to see whether it is possible to extract any spatial information from the time series. It will be shown that this is indeed possible by virtue of a newly introduced correlation function. This makes it, in principle, possible to represent maps with a delay or memory term in a time-time diagram (see below), even if a spatial interpretation is not directly possible. It should be noted here, that the 'spatial' dimension of the TDM in general does not coincide with the dimension of the system under consideration. An infinitely long CML is e.g. infinitely dimensional, although its spatial dimension might be as low as one.

The basic idea of the TDM consits of stretching the time axis of the CML and folding in the spatial dimensions one for one. That is to say, a multiple space-time rotation is performed. In one dimension it becomes

$$G(y_n(i)) = x_{i+(n-1)N}, \tag{1}$$

and in n dimensions,

$$G(y_n(i_k)) = x_T, \tag{2}$$

with

$$T = (n-1)\prod_{j=1}^{D} N(j) + \sum_{k=0}^{D-2}(i_{D-k}-1)\prod_{l=1}^{D-k-1} N(l) + i_1, \tag{3}$$

where $y_n(i_k)$ is the amplitude of lattice site i_k at time n, x_T the amplitude at time T, $N(j)$ the number of lattice points in direction j and D the spatial dimension of the lattice.

Transformation (2) is exact and reversible for all internal lattice sites. By internal lattice sites, those lattice sites whose coupling range does not exceed the boundary are meant. In general, it is not possible to include the boundary in a natural way. Below, it will be shown that, although slightly artificial, terms accounting for fixed boundary conditions or boundary conditions which are a function of their location can be included in (2). In such a case, a TDM and a CML are equivalent. It is impossible, however, to account for the popular periodic boundary conditions without taking the rather drastic measure of changing the coupling algorithm at set times.

In many situations, it is believed, though, that the boundary conditions do not play an essential role for the phenomenology of the system. Accordingly, one is free to chose the most simple or most transparent algorithm for a certain problem.

Let us first have a look at the one dimensional diffusively coupled logistic lattice which has become one of the paradigms of spatio-temporal chaos [8,9]:

$$y_{n+1}(i) = F\left((1-\epsilon)y_n(i) + \frac{\epsilon}{2}\left(y_n(i+1) + y_n(i-1)\right)\right), \tag{4}$$

where n is the discrete time, i the lattice site, ϵ the lattice coupling constant and $F(x_n)$, the logistic map, which is given by

$$F(x_n) = x_{n+1} = 1 - \alpha x_n^2, \tag{5}$$

with α a constant. The corresponding Time-Delayed Map, obtained with the help of (1), then looks like

$$x_n = (1-\epsilon)F(x_{n-N}) + \frac{\epsilon}{2}\left(F(x_{n-N-1}) + F(x_{n-N+1})\right). \tag{6}$$

If the exact transient time is not relevant, this is equivalent to

$$x_n = F\left((1-\epsilon)x_{n-N} + \frac{\epsilon}{2}\left(x_{n-N-1} + x_{n-N+1}\right)\right), \tag{7}$$

which immediately follows by applying F on both sides of Eq. (6), defining $x'_n = F(x_n)$ and dropping the prime. The time-delay N can also be considered to be the 'pseudo' system size, since a time-delay of N corresponds the closest to a CML with systemsize N.

As an illustration, a time-time and space-time diagram are shown in Fig. 1a) and 1b) respectively. The time-time diagram was constucted by placing slices of length N next to each other, in a way that is similar as to how a TV builds up an image. An entry was plotted black if the corresponding x_n or $y_n(i)$ was larger than the unstable fixed point $\frac{\sqrt{1+4\alpha}-1}{2\alpha}$ of the logistic map and the upper left corner is the origin. It can be clearly seen that in a phenomenological sense, the two graphs are extremely similar.

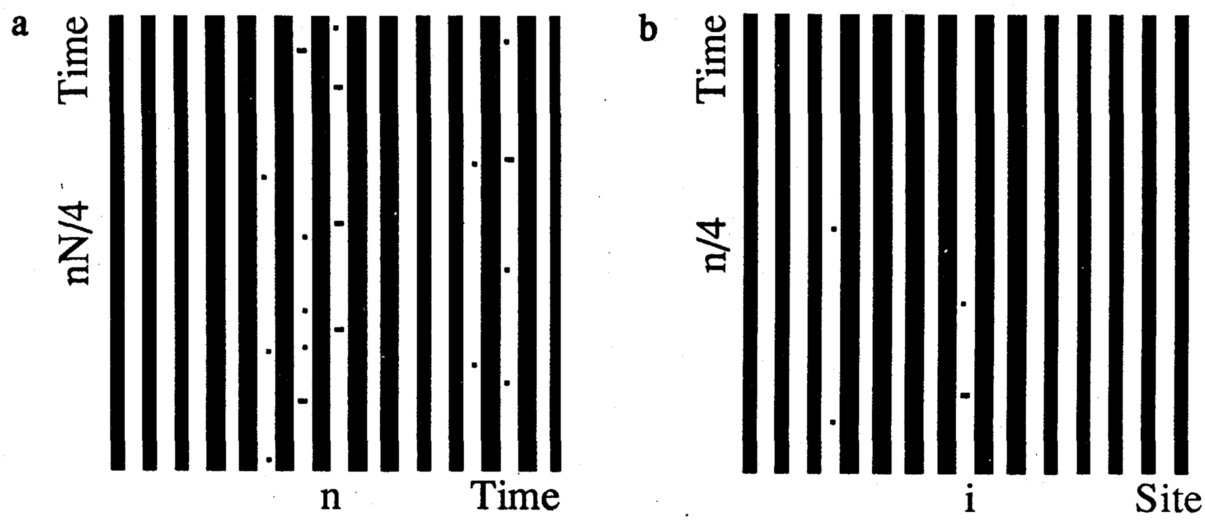

Figure 1: (a) Time-time diagram of the Pattern Slection Regime for the Time-Delayed Map, (b) Space-time diagram of the Pattern Selection Regime for a Coupled Map Lattice. In both cases the parameters were identical: $N = 100$, $\alpha = 1.7$ and $\epsilon = 0.4$.

The phenomenology of a TDM and a CML is, in general, not similar, though, when the boundary plays an essential role. This can be seen in Fig. 2, where the time-time and space-time diagrams of a TDM and CML respectively are displayed for the case of fixed initial conditions. For a TDM, a fixed inital condition, of course, means a fixed past. In Fig. 2a) the homogeneous initial slice in the y-direction is quickly destroyed, since information from the end of one slice is carried over to the beginning of the next one due to the lack of boundary conditions. In the case of a CML, fixed initial conditions effectively reduce the CML to a single logistic map. In the spatial direction, all lattice sites assume the same value yielding a bar-code like pattern in Fig. 2b).

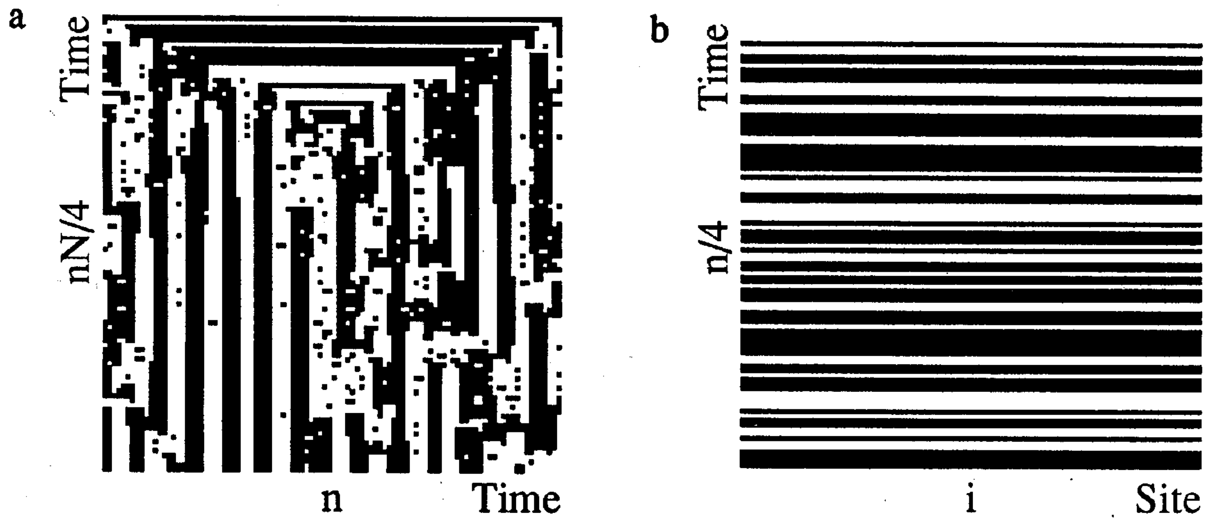

Figure 2: (a) Difference between a TDM and CML. Time-time diagram for the TDM and (b) Space-time diagram for the CML. In both cases, the parameters were identical: $\alpha = 1.7$, $\epsilon = 0.4$. The system size is $N = 100$ and the fixed initial condition was 0.0.

In the previous example, the equivalence between the TDM and CML was not exact. Next, let us have a look at a model where an exact transformation between the TDM and the CML representation can be found. It is a model for open fluid flow [10,11]. A Time-Delayed Map can be constructed by introducing a periodic interruption of the coupling algorithm. The model can be expressed as

$$\begin{aligned} x_n &= (1-\epsilon)F(x_{n-N}) + \epsilon F(x_{n-N-1}) - \\ &\quad [(1-\epsilon)F(x_{n-N}) + \epsilon F(x_{n-N-1}) - x^*]\,\delta(\mathrm{Mod}(n-1, N)), \end{aligned} \tag{8}$$

where n is again the discrete time, ϵ the coupling constant, N the time-delay and $F(x_n)$ the logistic map (5) . With the help of the space-time rotation

$$G(y_n(i)) = x_{i+(n-1)N} - \left(x_{i+(n-1)N} - x^*\right)\delta(i-1), \tag{9}$$

this can be mapped to the one-way CML

$$y_{n+1}(i) = (1-\epsilon)F(y_n(i)) + \epsilon F(y_n(i-1)). \tag{10}$$

The boundary condition is fixed and chosen to be

$$y_n(1) = x^*, \tag{11}$$

where x^* is again the unstable fixed point of the logistic map (5).

Some characteristics of the open fluid model are displayed in Fig. 3. Fig. 3a) shows a periodic temporal bifurcation. For the generation of this

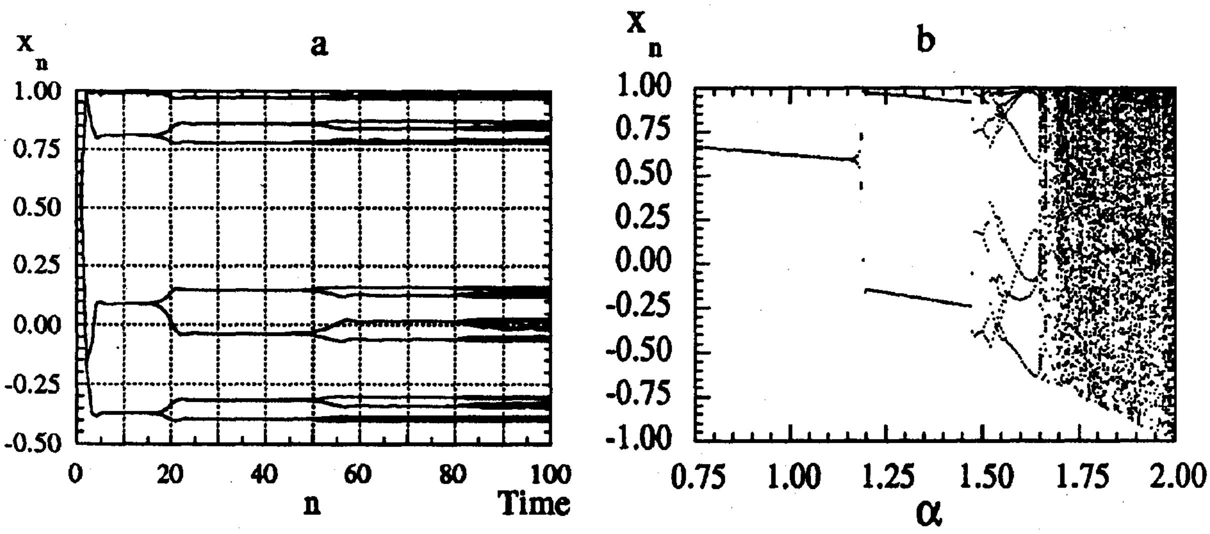

Figure 3: (a) Temporal bifurcation in a time-amplitude diagram. The system size is $N = 100$, $\alpha = 1.402$ and $\epsilon = 0.2$. One hundred slices of length N were overlaid. (b) Bifurcation diagram in α. The system size is $N = 100$, $\epsilon = 0.3$ and the post-delay is $j = 10$.

time-amplitude diagram one hundred slices of length N were overlaid. The bifurcations occur in what corresponds to the down flow direction. The increasing complexity of the system in that direction is also reflected in in the bifurcation diagram of Fig. 3b). The bifurcation parameter is the nonlinearity α and for every value of α 100 amplitudes x_{1+j+kN} were plotted, where N is the system size, k is an integer larger than zero and j the post-delay. The post-delay determines how far down flow the bifurcation diagram is constructed and can be viewed upon as the location of a probe in spatial terms or as the offset in time steps of a stroposcopic observation in temporal terms. The deformation of the bifurcation diagram can clearly be seen.

So far, two one dimensional systems were considered. The TDM for a two dimensional diffusively coupled logistic lattice with nearest neighbor interaction can be expressed as

$$\begin{aligned} x_n &= F\Big((1-\epsilon)x_{n-NM} + \\ &\quad \frac{\epsilon}{4}\left[x_{n-NM-1} + x_{n-NM+1} + x_{n-NM-N} + x_{n-NM+N}\right]\Big) \end{aligned} \tag{12}$$

where N and M were chosen to be the number of lattice points in the x and y direction respectively. In n dimensions this becomes

$$x_n = F\Big((1-\epsilon)x_{n-N_w} + \frac{\epsilon}{2D}\left[\sum_{i=0}^{D-1} x_{n-N_w-\prod_{j=0}^{i} N(j)} + x_{n-N_w+\prod_{j=0}^{i} N(j)}\right]\Big), \qquad (13)$$

where it is assumed that $\Pi_0^0 = 1$.

Two typical time-time patterns are displayed in Fig. 4. The x-axis represents the linear time and the y-axis the time modulo N. This time-time pattern corresponds to a snapshot of CML and is constructed with the help of $N \times M$ successive values of the time series generated by (12).

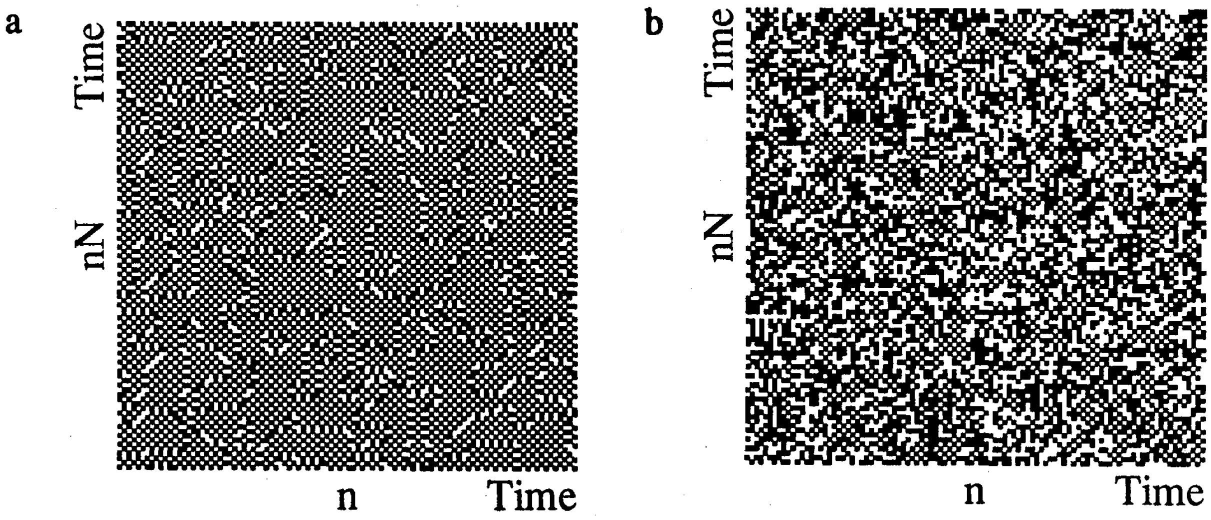

Figure 4: Time-time pattern of a two dimensional TDM. The system size is 100×100 and a transient of one million steps was discarded. (a) Brownian Motion of chaotically moving strings: $\alpha = 1.77$, $\epsilon = 0.1$. (b) Intermittency: $\alpha = 1.91$, $\epsilon = 0.1$.

Another interesting model uses a map with an excitable state as the local element. The Map

$$F(x) = b \times (x - \Theta(x)) + c, \qquad (14)$$

was originally introduced in connection with the firing of an artificial neuron [12]. $\Theta(x)$ is Heavisides step function, and b and c are real parameters. $F(x)$ is considered to be in an excited state if $x > 0$ and c represents an external stimulus. As in [8], c is taken to be the sum of what corresponds to nearest neighbors in a CML. In our TDM we obtain,

$$
\begin{aligned}
x_n \;=\;& b \times (x_{n-NM} - \Theta(x_{n-NM})) + \\
& d \times (\Theta(x_{n-NM-1}) + \Theta(x_{n-NM+1}) + \Theta(x_{n-NM-N}) + \Theta(x_{n-NM+N})) \,.
\end{aligned} \tag{15}
$$

This map exhibits BZ-like structures as can be seen in Fig. 5, where the time series is, as in the previous example, represented as a time-time diagram. There seem to be two types of patterns, self-sustained patterns and noise-

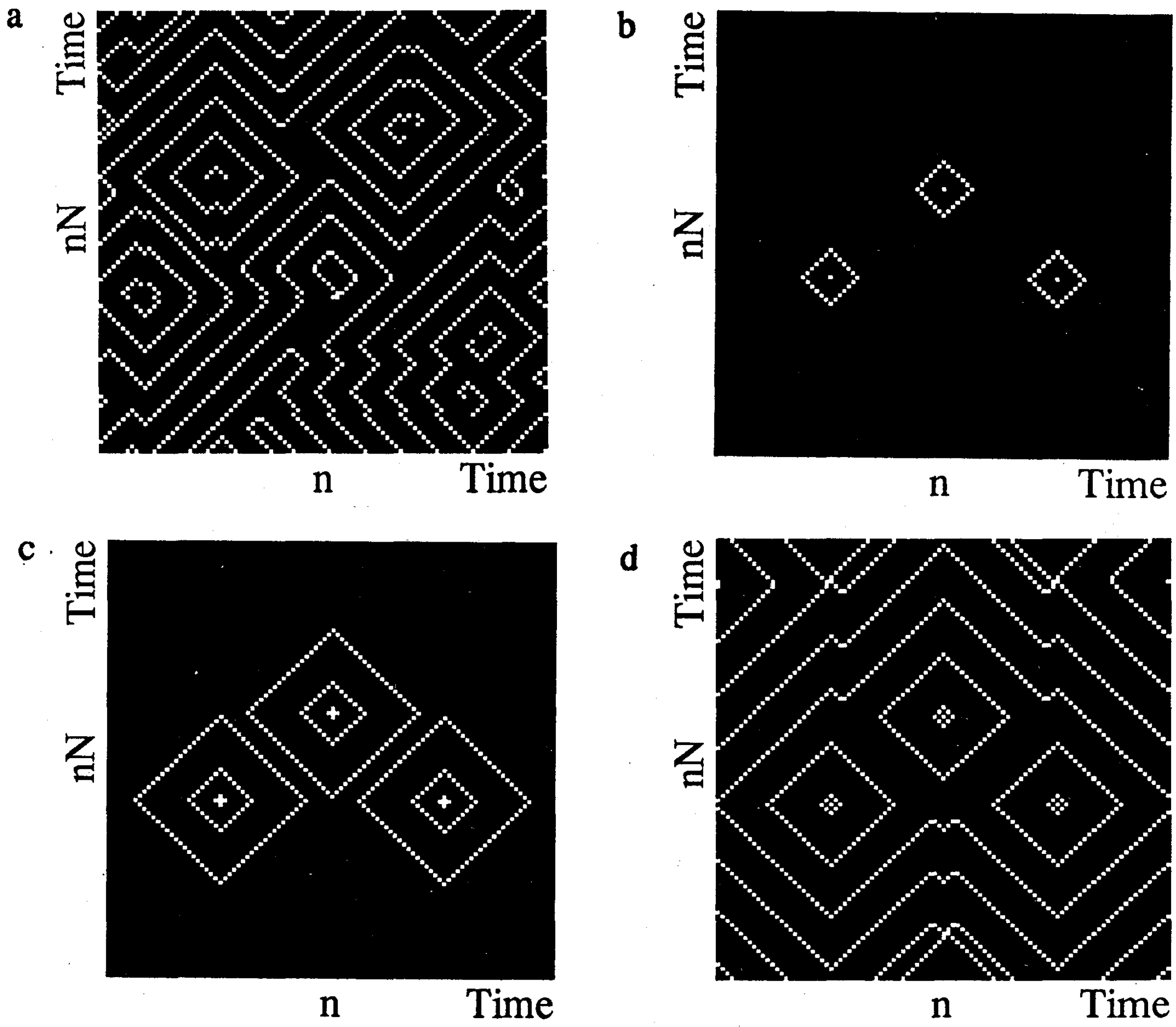

Figure 5: Time-time diagrams for an excitable media model. (a) Self-sustained pattern at time $T = 125N_w$; $b = 0.5$, $d = 0.0125$. (b), (c) and (d) Noise-sustained patterns at times $T = 12N_w$, $T = 25N_w$ and $T = 104N_w$; $b = 0.5$, $d = 0.0125$. The maximum amplitude of the positive noise was 0.05.

sustained ones. When starting with a random initial past, in general, a self-sustained pattern emerges. During the transient time, first almost all the points in the time series drops to a value close to zero. Then some points, modulo $M \times N$, become the seeds of outward moving waves. Fig. 5a) shows a typical self-sustained pattern after the transients have died out. Since a pattern consists of a slice of length $N \times M$, it is natural to use the 'pseudo' system size

$$N_w = NM \tag{16}$$

as the unit for the transient time. If one starts with an initial past fixed to zero and adds noise periodically, the points of the time series to which the noise is added become the seeds of a noise-sustained pattern. Again outward moving waves are created. A sequence of three patterns, Fig. 5b), c) and d), clearly shows the evolution of the system.

In Fig. 6, the wave forms, corresponding to the self-sustained and noise-sustained patterns respectively, are displayed. In both cases the shape of the 'dip' is similar. The wavelength, however is different. The wavelength of the self-sustained pattern is 8 time steps and the wavelength of the noise-sustained pattern is 12. Fig. 6a) corresponds to the bottom row of Fig. 5a)

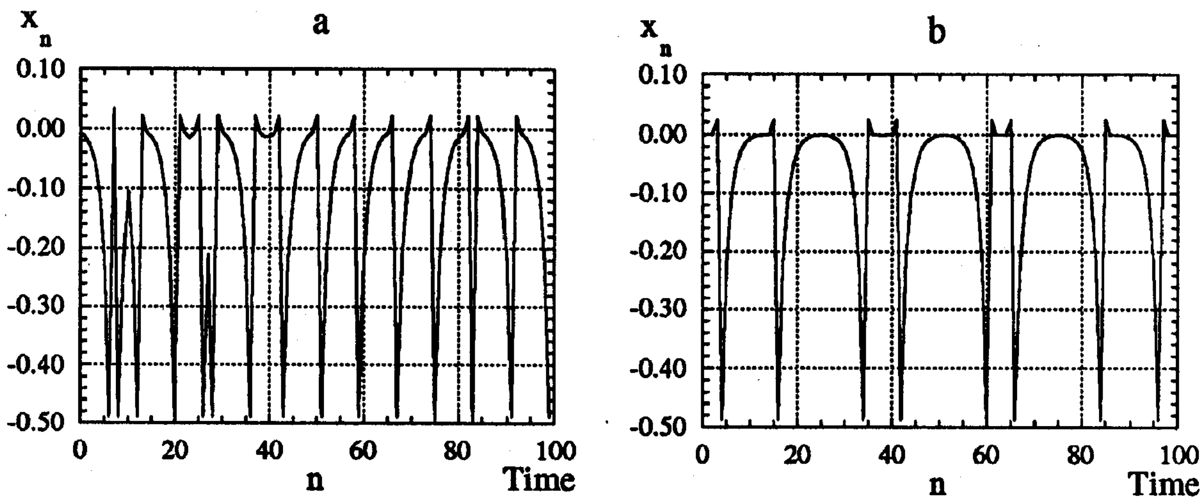

Figure 6: Waveforms corresponding to the patterns in Fig. 5. (a) The waveform of a self-sustained pattern. The parameters are the same as in Fig. 5a). (b) The waveform of a noise-sustained pattern. The parameters are the same as in Fig. 5d).

and Fig. 6b) corresponds to the bottom row of Fig. 5d). In (a), between time steps 43 and 83, five peaks can be seen that are moving to the left and between time steps 83 and 99, two peaks that are moving to the right. When two peaks that are moving into opposite directions meet, like around time step 40, they annihilate. In (b), although less clearly, the same can be seen for the longer wavelength.

Until now, it was shown how spatial information can be expressed in a time series. It would be intersting to see whether it is possible to extract this spatial information from the time series without a priori knowlegde of the system size. It is obvious from e.g. Fig. 1, that a clear correlation should exist between slices of length N. To retrieve the 'pseudo' system size N the following correlation function is introduced:

$$C(N) = -\frac{1}{L}\sum_{j=0}^{L}(x_{n-j} - x_{n-N-j})^2 \tag{17}$$

First let us apply (17) to a time series that corresponds to a Frozen Random Pattern and that was generated with (6). In that case we know what the answer should be. Although this example might seem trivial, it is not completely so since no information regarding the system size is passed to the correlation function.

In Fig. 7a), the distance between the large peaks clearly equals $\Delta N = 100$, the system size used for the generation of the time series. Looking at

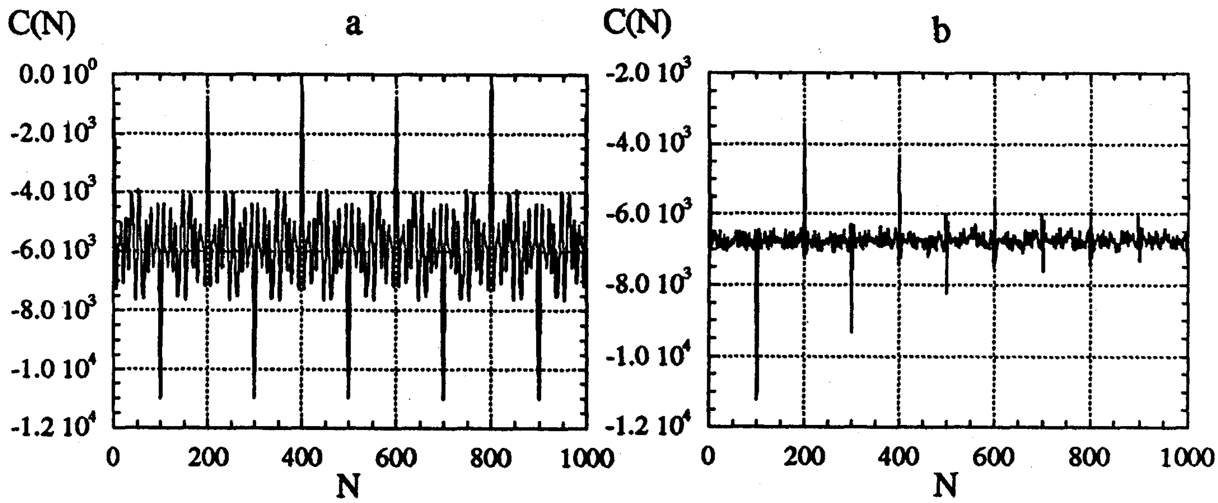

Figure 7: Correlation function. The peaks corresponding to the system size can clearly be seen. (a) In the Pattern Selection regime, $\alpha = 1.7$, $\epsilon = 0.4$. (b) In the Chaotic, high nonlinearity regime, $\alpha = 2.0$, $\epsilon = 0.3$

the seperate peaks, one can see that the correlation of every fourth peak assumes the same value, implying the existence of four phases. Hence, the correlation function indeed correctly extracts the desired information from the time series.

It should be noted here that a time series corresponding to a Frozen Pattern provides us with quite an ideal example to demonstrate (17). A single section, in general, cannot be translated by less than its length and yield an (almost) exact overlap with its untranslated origin. On the other hand, a slice and another slice N_w times the periodicity of the part with the longest periodicity of the slice in the future, have a very large correlation, yielding a sharp peak in the correlation function while minimizing 'false' peaks due to correlations within a slice. In the case of the Pattern Selection regime, e.g., the peaks in the correlation function are much less distinct while there are many smaller peaks. This is not a drawback, though, since this only reflects the fact that, at least in the stationary case, the effective system size of a pattern in the Pattern Selection regime equals the wavelength of that pattern.

In the case of a time series generated with the TDM (6), the correlation function (17) determines the correct system size even in regions of high nonlinearity where the system is considered to be chaotic. Surprisingly clear results were obtained even for the maximum nonlinearity $\alpha = 2.0$, as can be seen in Fig. 7b). For increasing N, the peaks decrease which is as expected since there shouldn't be any long time correlations in the chaotic regime.

Conclusions and Discussion. It was shown that a Time-Delayed Map can effectively model many spatio-temporal phenomena in any dimension. For certain types of boundary conditions an exact mapping to a Coupled Map Lattice can be established. If such an exact map does not exist while the boundary of the CML does not play an essential role for the phenomenology of a model, the phenomenology of a TDM and a CML can be considered to be identical. The construction of the TDM is, especially in more than one dimension, not as transparent as the one of a CML. Future research will have to show whether this disadvantage is offset by its more straigthforward coupling algorithm.

The newly introduced correlation function, however, which is quite natural in the context of a TDM but rather unnatural in the context of a CML, has revealed that, even in the region of maximum nonlinearity, the system size can be extracted from a chaotic time series. It will be interesting to see whether the correlation function can be applied to the data of a probe placed in a spatially extended system. Since such a system would almost certainly be continous, it might also provide us with information on how large a lattice that simulates the system should be. Although the application of the correlation function to a system with some kind of intrinsic spatial lengthscale seems to be the most natural, it could also be used for the analysis of time series where a spatial interpretation is not obvious. In that case, it would provide the proper 'system size' for the generation of a time-time diagram which might assist in visualizing (recurrent) patterns in a time series that are otherwise hard to detect.

Last but not least, one could apply it to a CML with the help of the space-time rotation (2). (At least in some cases) an 'effective' kind of dimension could then be obtained by taking the Fourier transform of $C(N)$. Whether this indeed yields any tangible results is under present investigation and the outcome will be included in a future publication.

acknowledgements

The author would like to thank Dr. K. Kaneko and Dr. K. Nemoto for many valuable discussions, and Dr. H. Takayama and Dr. T. Arimitsu for their continous support.

References

[1] K. Kaneko [1984], 'Period-Doubling of Kink-Antikink Patterns, Quasiperiodicity in Antiferro-Like Structures and Spatial Intermittency in Coupled Map Lattice', Prog. Theor. Phys. 72, 480

[2] J.P. Crutchfield and K. Kaneko [1987], 'Phenomenology of Spatiotemporal Chaos' in *Directions in Chaos* (World Scientific)

[3] J.D. Farmer [1982], 'Chaotic Attractors of an Infinite-Dimensional Dynamical System', Physica 4D, 366

[4] F.H. Willeboordse [1992], 'Time-Delayed Map, Phenomenological Equivalence with a Coupled Map Lattice', to appear in the International Journal of Bifurcation and Chaos.

[5] F.H. Willeboordse [1992], 'Time-Delayed Map, as a model for open fluid flow', submitted to Chaos.

[6] F.H. Willeboordse [1992], 'Time-Delayed Map, Extension to n Dimensions', to appear in Chaos, Fractals and Solitons.

[7] M. Giona [1991], 'Dynamics and Relaxation Properties of Complex Systems with Memory', Nonlinearity 4, 911

[8] K. Kaneko [1990], 'Simulating Physics with Coupled Map Lattices' in *Formation, Dynamics and Statistics of Patterns*, 1 (ed. K. Kawasaki, A. Onuki, and M. Suzuki, World Sci.)

[9] K. Kaneko [1989], 'Pattern Dynamics in Spatiotemporal Chaos', Physica 34D, 1

[10] K. Kaneko [1985], 'Spatial Period Doubling in Open Flow', Phys. Lett. 111, 321

[11] R. Deissler and K. Kaneko [1987], 'Velocity-Dependent Lyapounov Exponents as a Measure of Chaos for Open Flow Systems', Phys. Lett. 119A, 397

[12] J. Nagumo and S. Sato [1972], 'On a Response Characteristic of a Mathematical Neuron Model', Kybernetic 10, 155